



AIRBUS



RÉGION
**Nouvelle-
Aquitaine**

Direct solution of larger coupled sparse/dense FEM/BEM linear systems using low-rank compression

Sparse Days

Emmanuel Agullo, Marek Felšöci, Guillaume Sylvand

June 20 - 22, 2022

Inria Bordeaux Sud-Ouest, France

Team-project CONCACE

AIRBUS

- study the propagation of sound waves emitted by an aircraft
 - acoustic pollution reduction, prototype certification
- discrete model for numerical simulations
 - volume domain V (jet flow)
 - Finite Elements Method (FEM) [11, 9]
 - surface domain S (surface of the aircraft and the volume domain)
 - Boundary Elements Method (BEM) [6, 13]



An acoustic wave (blue arrow) emitted by the aircraft's engine, reflected on the wing and crossing the jet flow. Real-life case [12] (left) and a numerical model example (right).

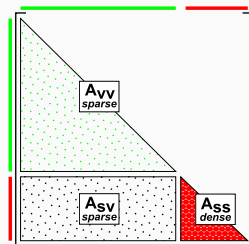
Problem

Global linear system coupling [7, 8] the FEM and the BEM unknowns:

$$\begin{bmatrix} A_{VV} & A_{SV}^T \\ A_{SV} & A_{SS} \end{bmatrix} \times \begin{bmatrix} x_V \\ x_S \end{bmatrix} = \begin{bmatrix} b_V \\ b_S \end{bmatrix}$$



- symmetric coefficient matrices:
 - sparse parts - volume domain V discretization with FEM (A_{VV}), surface/volume domain interaction (A_{SV})
 - a dense part - surface domain S discretization with BEM (A_{SS})
- finer model \rightarrow larger system
- direct solution using Schur complement [14]



Direct solution

Schur complement

- reduce the problem on boundaries \rightarrow simplify the system to solve

$$\begin{matrix} R_1 \\ R_2 \end{matrix} \begin{matrix} \text{green} & \text{red} \\ \left[\begin{array}{cc} A_{VV} & A_{SV}^T \\ A_{SV} & A_{SS} \end{array} \right] \end{matrix} \times \begin{bmatrix} x_V \\ x_S \end{bmatrix} = \begin{bmatrix} b_V \\ b_S \end{bmatrix}$$

Computation steps

1. eliminate x_V from the second equation \rightarrow Schur complement S

$$\begin{matrix} R_1 \\ R_2 \leftarrow R_2 - A_{SV} A_{VV}^{-1} \times R_1 \end{matrix} \begin{bmatrix} A_{VV} & A_{SV}^T \\ 0 & \underbrace{A_{SS} - A_{SV} A_{VV}^{-1} A_{SV}^T}_S \end{bmatrix} \times \begin{bmatrix} x_V \\ x_S \end{bmatrix} = \begin{bmatrix} b_V \\ b_S - A_{SV} A_{VV}^{-1} b_V \end{bmatrix}$$

2. solve the reduced Schur complement system

$$S x_S = b_S - A_{SV} A_{VV}^{-1} b_V$$

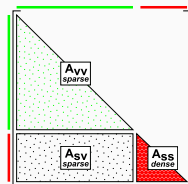
3. determine x_V using x_S

$$x_V = A_{VV}^{-1} (b_V - A_{SV}^T x_S)$$

Numerical computation

Properties of the input linear system

- A_{VV} and A_{SS} are symmetric
- A_{VV} and A_{SV} are sparse



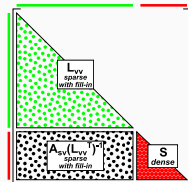
Initial state of A

Ideal computation of $S = A_{SS} - A_{SV}A_{VV}^{-1}A_{VS}$

- symmetric factorization of $A_{VV} \rightarrow L_{VV}L_{VV}^T$: fill-in

$$S = A_{SS} - A_{SV}(L_{VV}L_{VV}^T)^{-1}A_{SV}^T$$

- computation of the Schur complement



A after computing S

$$S = A_{SS} - \underbrace{(A_{SV}(L_{VV}^T)^{-1})}_{\text{triangular solve}} \underbrace{(A_{SV}(L_{VV}^T)^{-1})^T}_{\text{implicitly known}}$$

Implementation

- coupling of a **sparse** direct and a **dense** direct solver
 - fully-featured community solvers with appealing functionalities
 - low-rank compression, out-of-core, distributed memory parallelism
- two different schemes depending on the way of using the building blocks of the **sparse** solver
 - *baseline* coupling
 - *advanced* coupling

Vanilla solver couplings

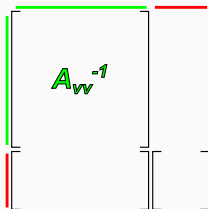
baseline coupling

- separate A_{VV} , A_{SV} and A_{SS}
- *sparse facto.*, *sparse solve*
- *dense facto.*, *dense solve*

Vanilla solver couplings

baseline coupling

- separate A_{VV} , A_{SV} and A_{SS}
- *sparse facto.*, *sparse solve*
- *dense facto.*, *dense solve*



Vanilla solver couplings

baseline coupling

- separate A_{vv} , A_{sv} and A_{ss}
- *sparse facto.*, *sparse solve*
- *dense facto.*, *dense solve*

The diagram illustrates a block matrix structure, likely representing a system of equations. It consists of two main vertical blocks enclosed in large square brackets. The left block is labeled A_{vv}^{-1} in green. The right block is labeled A_{sv}^T in black. A green horizontal line connects the top of the left block to the top of the right block. A red horizontal line connects the bottom of the left block to the bottom of the right block. Additionally, a green vertical line is on the left side of the left block, and a red vertical line is on the left side of the right block.

Vanilla solver couplings

baseline coupling

- separate A_{vv} , A_{sv} and A_{ss}
- *sparse facto.*, *sparse solve*
- *dense facto.*, *dense solve*

The diagram shows a block matrix structure represented by two large square brackets. The top-left block is labeled A_{vv}^{-1} in green. The top-right block is labeled A_{sv}^T in black. The bottom-right block is labeled S in red. A green vertical line is on the left of the first column, and a red vertical line is on the left of the second column. A green horizontal line is above the first column, and a red horizontal line is above the second column.

Vanilla solver couplings

baseline coupling

- separate A_{vv} , A_{sv} and A_{ss}
- *sparse facto.*, *sparse solve*
- *dense facto.*, *dense solve*

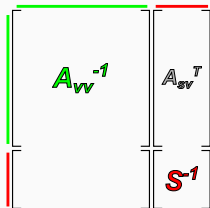
The diagram shows a block matrix structure with two columns and two rows of blocks. The top-left block is labeled A_{vv}^{-1} in green. The top-right block is labeled A_{sv}^T in black. The bottom-right block is labeled S^{-1} in red. A green vertical line is on the left of the first column, and a red vertical line is on the left of the second column. A green horizontal line is above the first column, and a red horizontal line is above the second column.

$$\begin{bmatrix} A_{vv}^{-1} & A_{sv}^T \\ & S^{-1} \end{bmatrix}$$

Vanilla solver couplings

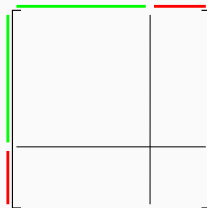
baseline coupling

- separate A_{vv} , A_{sv} and A_{ss}
- *sparse facto.*, *sparse solve*
- *dense facto.*, *dense solve*



advanced coupling

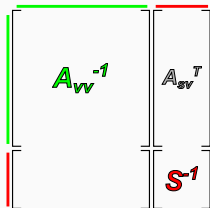
- A as a whole
- *sparse facto.* + *Schur*
- *dense facto.*, *dense solve*



Vanilla solver couplings

baseline coupling

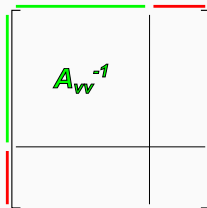
- separate A_{vv} , A_{sv} and A_{ss}
- *sparse facto.*, *sparse solve*
- *dense facto.*, *dense solve*



A diagram of a block matrix representing the baseline coupling. The matrix is partitioned into four quadrants. The top-left quadrant is labeled A_{vv}^{-1} in green. The top-right quadrant is labeled A_{sv}^T in black. The bottom-right quadrant is labeled S^{-1} in red. The matrix is enclosed in large square brackets. A green vertical line is on the left, and a red vertical line is on the right. A green horizontal line is at the top, and a red horizontal line is at the bottom.

advanced coupling

- A as a whole
- *sparse facto.*+Schur
- *dense facto.*, *dense solve*



A diagram of a block matrix representing the advanced coupling. The matrix is partitioned into four quadrants. The top-left quadrant is labeled A_{vv}^{-1} in green. The other three quadrants are empty. The matrix is enclosed in large square brackets. A green vertical line is on the left, and a red vertical line is on the right. A green horizontal line is at the top, and a red horizontal line is at the bottom.

Vanilla solver couplings

baseline coupling

- separate A_{vv} , A_{sv} and A_{ss}
- *sparse facto.*, *sparse solve*
- *dense facto.*, *dense solve*

A block matrix structure for baseline coupling. It consists of two columns. The first column contains a block A_{vv}^{-1} (green text) and an empty block below it. The second column contains a block A_{sv}^T (black text) and a block S^{-1} (red text) below it. A green vertical line is on the left of the first column, and a red vertical line is on the left of the second column. A green horizontal line is above the first column, and a red horizontal line is above the second column.

advanced coupling

- A as a whole
- *sparse facto.*+Schur
- *dense facto.*, *dense solve*

A block matrix structure for advanced coupling. It consists of two columns. The first column contains a block A_{vv}^{-1} (green text) and an empty block below it. The second column contains an empty block above a block S (red text). A green vertical line is on the left of the first column, and a red vertical line is on the left of the second column. A green horizontal line is above the first column, and a red horizontal line is above the second column.

Vanilla solver couplings

baseline coupling

- separate A_{vv} , A_{sv} and A_{ss}
- *sparse facto.*, *sparse solve*
- *dense facto.*, *dense solve*

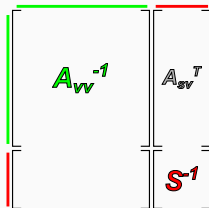


Diagram illustrating the baseline coupling structure. The matrix is partitioned into four blocks: A_{vv}^{-1} (top-left, green), A_{sv}^T (top-right, black), a zero block (bottom-left, black), and S^{-1} (bottom-right, red). The top row is highlighted with a green bracket, and the bottom row is highlighted with a red bracket.

advanced coupling

- A as a whole
- *sparse facto.*+Schur
- *dense facto.*, *dense solve*

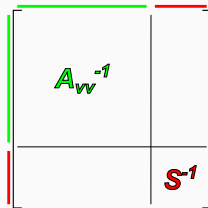
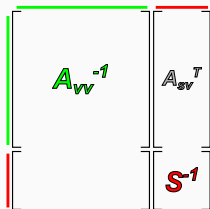


Diagram illustrating the advanced coupling structure. The matrix is partitioned into four blocks: A_{vv}^{-1} (top-left, green), a zero block (top-right, black), a zero block (bottom-left, black), and S^{-1} (bottom-right, red). The top row is highlighted with a green bracket, and the bottom row is highlighted with a red bracket.

Vanilla solver couplings

baseline coupling

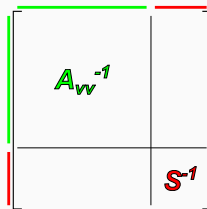
- separate A_{vv} , A_{sv} and A_{ss}
- *sparse facto.*, *sparse solve*
- *dense facto.*, *dense solve*



The diagram shows a block matrix structure for the baseline coupling. It consists of two columns. The first column has a green vertical line on its left and a red vertical line on its right. The second column has a red vertical line on its left. The top-left block is labeled A_{vv}^{-1} in green. The top-right block is labeled A_{sv}^T in black. The bottom-right block is labeled S^{-1} in red. The matrix is enclosed in large square brackets.

advanced coupling

- A as a whole
- *sparse facto.*+Schur
- *dense facto.*, *dense solve*



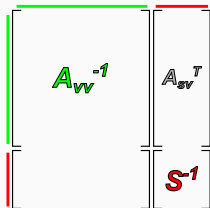
The diagram shows a block matrix structure for the advanced coupling. It consists of two columns. The first column has a green vertical line on its left and a red vertical line on its right. The second column has a red vertical line on its left. The top-left block is labeled A_{vv}^{-1} in green. The bottom-right block is labeled S^{-1} in red. The matrix is enclosed in large square brackets.

- S non-compressed, dense
- A_{sv}^T explicitly stored, dense

Vanilla solver couplings

baseline coupling

- separate A_{vv} , A_{sv} and A_{ss}
- *sparse facto.*, *sparse solve*
- *dense facto.*, *dense solve*

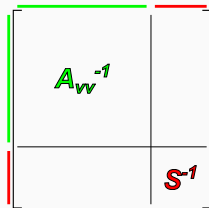


The diagram shows a block matrix structure for the baseline coupling. It consists of two columns. The first column has a green vertical line on its left and a red vertical line on its right. The second column has a red vertical line on its right. The top-left block is labeled A_{vv}^{-1} in green. The top-right block is labeled A_{sv}^T in black. The bottom-right block is labeled S^{-1} in red. The matrix is enclosed in large square brackets.

- S non-compressed, dense
- A_{sv}^T explicitly stored, dense

advanced coupling

- A as a whole
- *sparse facto.* + *Schur*
- *dense facto.*, *dense solve*



The diagram shows a block matrix structure for the advanced coupling. It consists of two columns. The first column has a green vertical line on its left and a red vertical line on its right. The second column has a red vertical line on its right. The top-left block is labeled A_{vv}^{-1} in green. The bottom-right block is labeled S^{-1} in red. The matrix is enclosed in large square brackets.

- S non-compressed, dense

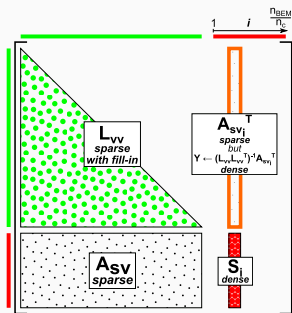
Coping with limitations

- keep using fully-featured well optimized community solvers despite limitations in their API
- two new algorithms for block-wise computation of S
 - allow for low-rank compression of S
 - 1. **multi-solve** based on the *baseline* coupling
 - 2. **multi-factorization** based on the *advanced* coupling

Multi-solve

$$S_i = A_{ss_i} - A_{sv} \overbrace{(L_{vv} L_{vv}^T)^{-1} A_{sv_i}^T}^{\text{solve} \rightarrow Y_i}$$

- 1 *sparse* facto. of the **green** matrix (symmetric)
- plenty of *sparse solve* involving the **orange** blocks (result is dense)

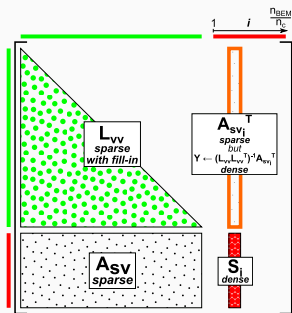


WITHOUT compression

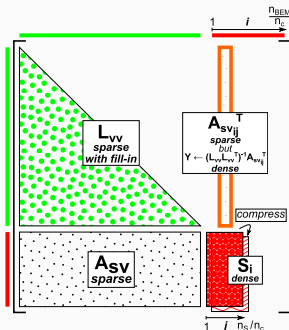
Multi-solve

$$S_i = A_{ss_i} - A_{sv} \overbrace{(L_{vv} L_{vv}^T)^{-1} A_{sv}^T}^{\text{solve} \rightarrow Y_i}$$

- 1 *sparse facto.* of the **green** matrix (symmetric)
- plenty of *sparse solve* involving the **orange** blocks (result is dense)



WITHOUT compression

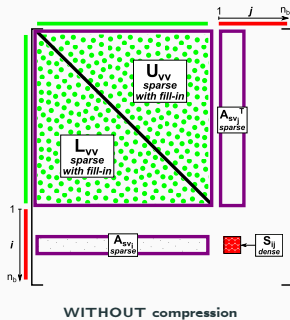


WITH compression

Multi-factorization

$$S_{ij} = A_{ssij} - \overbrace{A_{sv_i} (L_{vv} U_{vv})^{-1} A_{sv_j}^T}^{\text{used with Schur API}}$$

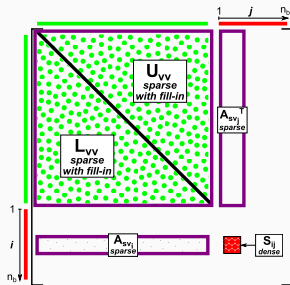
- multiple *sparse facto.* + *Schur* of the **violet** matrix (non-symmetric)
- computation of the Schur complement blocks via API



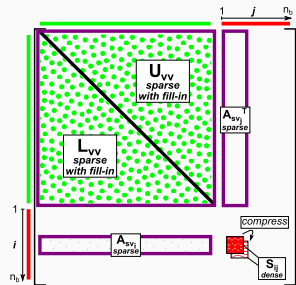
Multi-factorization

$$S_{ij} = A_{ssij} - \overbrace{A_{sv_i} (L_{vv} U_{vv})^{-1} A_{sv_j}^T}^{\text{used with Schur API}}$$

- multiple *sparse facto.* + Schur of the **violet** matrix (non-symmetric)
- computation of the Schur complement blocks via API



WITHOUT compression

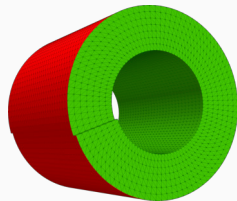


WITH compression

Experimental evaluation

Academic test case

- short pipe (length: 2 m, radius: 4 m) [3]
- systems close enough to real-life models
- FEM/BEM mesh (v and s parts)



A short pipe (20,000 unknowns)

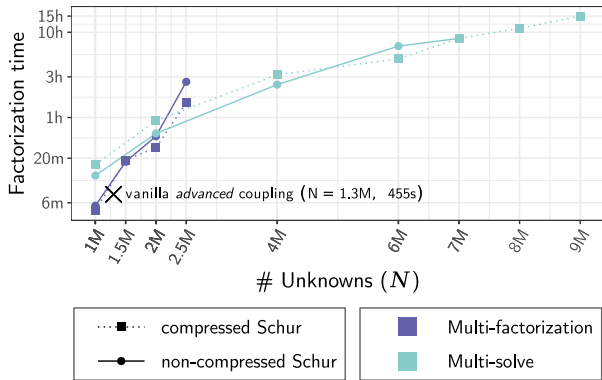
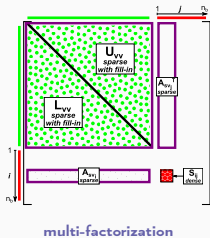
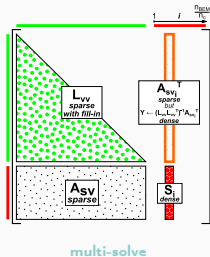
Configuration

- PlaFRIM [1], 24-core *miriel* nodes
 - 128 GiB of RAM
- precision parameter ϵ set to 10^{-3}
- sparse solver with low-rank compression always on
- out-of-core disabled

Implementation

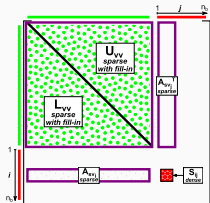
- sparse solver
 - MUMPS [4]
- dense solvers
 - SPIDO
(non-compressed S)
 - HMAT
(compressed S) [10]

Solving larger systems

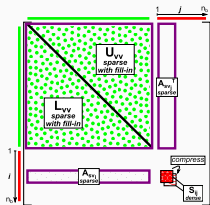


Best computation times of multi-solve and multi-factorization for both solver couplings, MUMPS/HMAT (compressed Schur) and MUMPS/SPIDO (non-compressed Schur). Parallel runs using 24 threads on single *miriel* node.

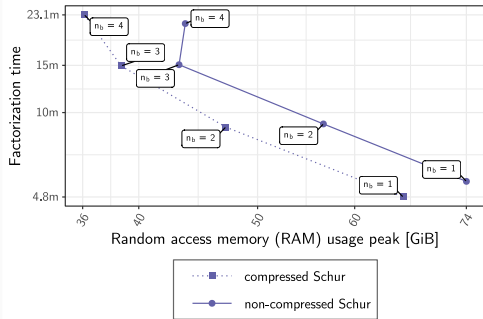
Performance-memory trade-off of multi-factorization



multi-factorization
(non-compressed)



multi-factorization
(compressed)

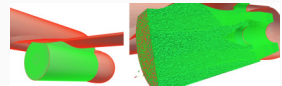


Comparison between the non-compressed and compressed multi-factorization for the MUMPS/HMAT (compressed Schur) and the MUMPS/SPIDO (non-compressed Schur) couplings on a coupled FEM/BEM system with system with 1,000,000 unknowns for varying n_b .

Industrial application

Industrial test case

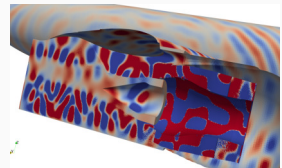
- 2,259,468 unknowns
 - 2,090,638 in the **v** part
 - 168,830 in the **s** part
- 32-core machine with 384 GiB of RAM



Model FEM/BEM mesh

Results

Algorithm	RAM (GiB)	Time
vanilla <i>advanced</i> coupling	>384	N/A
multi-solve (non-compressed S)	224	15h
multi-factorization (non-compressed S)	275	8h
multi-solve (compressed S)	35	9h
multi-factorization (compressed S)	137	51m



Computed acoustic pressure

Contribution

- two algorithms allowing us to:
 - benefit from the most advanced functionalities of fully-featured solvers
 - process larger systems compared to vanilla couplings
 - 9M (**multi-solve**) and 2.5M (**multi-factorization**) vs. 1.3M on a single 24-core, 128 GiB RAM workstation
 - industrial case impossible to run before on a single 32-core, 384 GiB RAM workstation
- confirm the advantage of compressing the Schur complement
- validate the algorithms on a real-life industrial case

Ongoing work

- extension to out-of-core and distributed memory cases

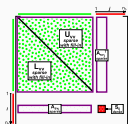
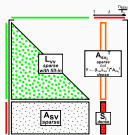
Towards ideal implementation

Main limitations

- multi-solve - explicit storage of dense orange blocks
- multi-factorization - re-factorizations of the green matrix

Collaboration with A. Buttari (IRIT/ENSEEIH)

- coupling of task based direct solvers
 - sparse: qr_mumps [2]
 - no compression, no distributed memory parallelism
 - dense: HMAT
 - relying on the StarPU runtime [5]
 - built-in out-of-core capability
- S is never assembled entirely in memory
- dense solver can start working without waiting for S to be fully assembled



multi-
factorization

Thank you for attending!

Looking for a post-doctoral research position
(Ph.D. defense expected in January 2023)

Acknowledgement

- Projet Région Nouvelle-Aquitaine 2018-1R50119
« HPC scalable ecosystem »
- PlaFRIM experimental testbed [1] (supported by Inria, CNRS - LABRI and IMB, Université de Bordeaux, Bordeaux INP and Conseil Régional d'Aquitaine)

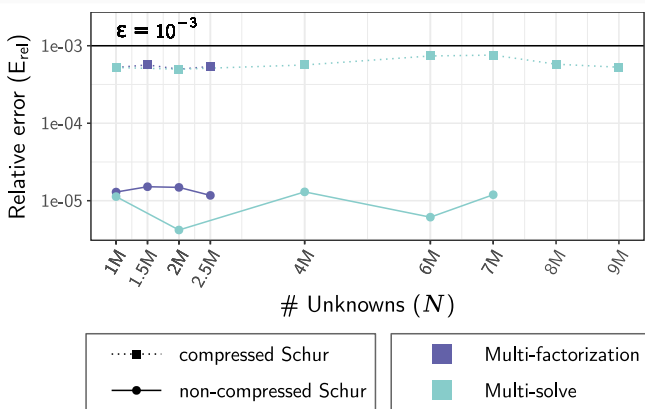
- [1] *PlaFRIM: Plateforme fédérative pour la recherche en informatique et mathématiques.*
<https://plafrim.fr/>.
- [2] *qr_mumps, a software package for the solution of sparse, linear systems on multicore computers.*
http://buttari.perso.enseeiht.fr/qr_mumps/.
- [3] *test_FEMBEM, a simple application for testing dense and sparse solvers with pseudo-FEM or pseudo-BEM matrices.*
https://gitlab.inria.fr/solverstack/test_fembem.
- [4] P. R. Amestoy, I. S. Duff, and J.-Y. L'Excellent, *MUMPS multifrontal massively parallel solver version 2.0*, (1998).

- [5] C. Augonnet, S. Thibault, and R. Namyst, *StarPU: a Runtime System for Scheduling Tasks over Accelerator-Based Multicore Machines*, Rapport de recherche RR-7240, INRIA, Mar. 2010.
- [6] P. K. Banerjee and R. Butterfield, *Boundary element methods in engineering science*, vol. 17, McGraw-Hill London, 1981.
- [7] F. Casenave, *Méthodes de réduction de modèles appliquées à des problèmes d'aéroacoustique résolus par équations intégrales*, PhD thesis, Université Paris-Est, 2013.
- [8] F. Casenave, A. Ern, and G. Sylvand, *Coupled BEM–FEM for the convected Helmholtz equation with non-uniform flow in a bounded domain*, Journal of Computational Physics, 257 (2014), pp. 627–644.
- [9] A. Ern and J.-L. Guermond, *Theory and practice of finite elements*, vol. 159, Springer Science & Business Media, 2013.

- [10] B. Lizé, *Résolution Directe Rapide pour les Éléments Finis de Frontière en Électromagnétisme et Acoustique : \mathcal{H} -Matrices. Parallélisme et Applications Industrielles.*, PhD thesis, Université Paris 13, 2014.
- [11] P. Raviart and J. Thomas, *A mixed finite element method for 2-nd order elliptic problems*, in Mathematical Aspects of Finite Element Methods, I. Galligani and E. Magenes, eds., vol. 606 of Lecture Notes in Mathematics, Springer Berlin Heidelberg, 1977, pp. 292–315.
- [12] Sebaso, *Jet engine airflow during take-off*.
https://commons.wikimedia.org/wiki/File:20140308-Jet_engine_airflow_during_take-off.jpg.

- [13] A. Wang, N. Vlahopoulos, and K. Wu, *Development of an energy boundary element formulation for computing high-frequency sound radiation from incoherent intensity boundary conditions*, Journal of Sound and Vibration, 278 (2004), pp. 413–436.
- [14] F. Zhang, *The Schur complement and its applications*, vol. 4, Springer Science & Business Media, 2006.

Numerical assessment

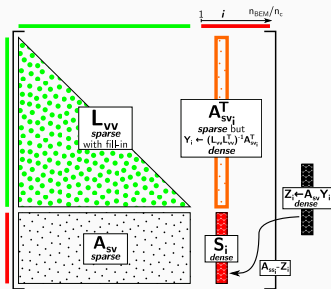


Relative error E_{rel} for the runs of **multi-solve** and **multi-factorization** having the best execution times and for both solver couplings, MUMPS/HMAT (compressed Schur) and MUMPS/SPIDO (non-compressed Schur). Parallel runs using 24 threads on single *miriel* node.

Multi-solve

$$S_i = A_{ss_i} - \underbrace{A_{sv} \underbrace{(L_{vv} L_{vv}^T)^{-1} A_{sv}^T}_{Z_i}}_{\text{solve} \rightarrow Y_i}$$

- 1 *sparse facto.* of the **green** matrix (symmetric)
- plenty of *sparse solve* involving the **orange** blocks (result is dense)

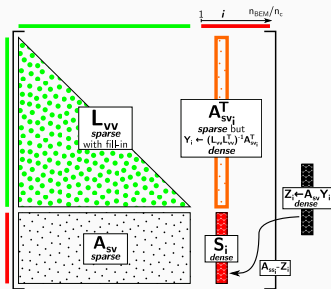


WITHOUT compression

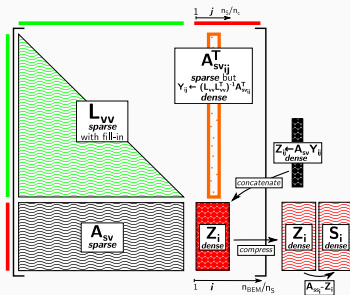
Multi-solve

$$S_i = A_{ss_i} - \underbrace{A_{sv} \underbrace{(L_{vv} L_{vv}^T)^{-1} A_{sv}^T}_{Z_i}}_{\text{solve} \rightarrow Y_i}$$

- 1 *sparse facto.* of the **green** matrix (symmetric)
- plenty of *sparse solve* involving the **orange** blocks (result is dense)



WITHOUT compression



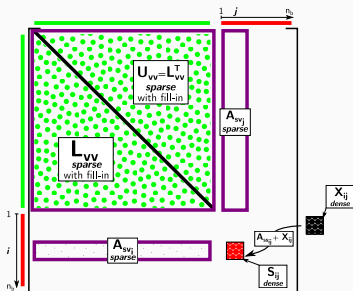
WITH compression

Multi-factorization

used with Schur API $\rightarrow X_{ij}$

$$S_{ij} = A_{ssij} - \overbrace{A_{svi} (L_{vv} U_{vv})^{-1} A_{svj}^T}$$

- multiple *sparse facto.* + *Schur* of the **violet** matrix (non-symmetric)
- computation of the Schur complement blocks via API

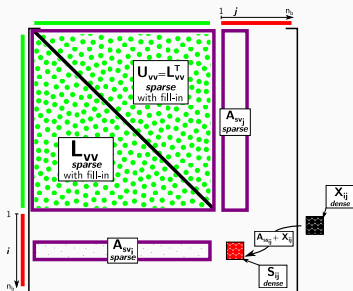


Multi-factorization

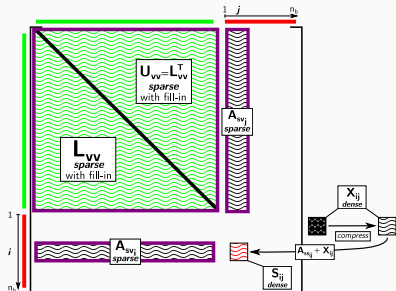
used with Schur API $\rightarrow X_{ij}$

$$S_{ij} = A_{ssij} - \overbrace{A_{svi}(L_{vv}U_{vv})^{-1}A_{svj}^T}^{X_{ij}}$$

- multiple *sparse facto.+Schur* of the **violet** matrix (non-symmetric)
- computation of the Schur complement blocks via API



WITHOUT compression



WITH compression